Monte Carlo ray-tracing simulations of luminescent solar concentrators for building integrated photovoltaics

Shin Woei Leow[a,b], Carley Corrado[a], Melissa Osborn[a], Sue A. Carter[a]
[a]Dept. of Physics, Univ. of California, Santa Cruz, CA USA 95064; [b]Jack Baskin Sch. of Engineering, Univ. of California, Santa Cruz, CA USA 95064

ABSTRACT

Luminescent solar concentrators (LSCs) have the ability to receive light from a wide range of angles, concentrating the captured light onto small photo active areas. This enables greater incorporation of LSCs into building designs as windows, skylights and wall claddings in addition to rooftop installations of current solar panels. Using relatively cheap luminescent dyes and acrylic waveguides to effect light concentration onto lesser photovoltaic (PV) cells, there is potential for this technology to approach grid price parity. We employ a panel design in which the front facing PV cells collect both direct and concentrated light ensuring a gain factor greater than one. This also allows for flexibility in determining the placement and percentage coverage of PV cells during the design process to balance reabsorption losses against the power output and level of light concentration desired. To aid in design optimization, a Monte-Carlo ray tracing program was developed to study the transport of photons and loss mechanisms in LSC panels. The program imports measured absorption/emission spectra and transmission coefficients as simulation parameters with interactions of photons in the panel determined by comparing calculated probabilities with random number generators. LSC panels with multiple dyes or layers can also be simulated. Analysis of the results reveals optimal panel dimensions and PV cell layouts for maximum power output for a given dye concentration, absorbtion/emission spectrum and quantum efficiency.

Keywords: photovoltaics, solar energy concentrators, solar cells, luminescent dyes, Monte-Carlo, ray-tracing, Building integrated photovoltaics

1. INTRODUCTION

The high energy needs and dense urban environment of many modern cities extracts a toll on the environment and natural resources available. Building integrated photovoltaics (BIPV) offers a viable method for harvesting additional solar energy utilizing existing building space, by enabling the expansion of PV module installation onto walls and windows[1–3]. While advancements in PV cell technology continuous to boost energy conversion efficiency and lower cost, grid parity has yet to be achieved. LSCs are static non-imaging type solar concentrators and thus are basic in their construct, providing a simple and low cost method in which to implement BIPV. Fluorescent dyes embedded in a waveguide absorb and redirect incident light into the waveguide. A portion of this light remains trapped within via total internal reflection thereby concentrating the light until it is collected by PV cells optically coupled to the waveguide. This ability to redirect light grants LSC panels the capacity to absorb both direct and diffuse light negating the need for expensive solar tracking systems[4–8]. Adjustments to dye mixture and concentration to achieve color tuning and partial transparency extends the application of LSC technology to the construction of windows, skylights and greenhouse panels beyond the usual roof installations.

While there exists many types of luminescent dyes, none are endowed with all the qualities needed for an ideal LSC panel. Issues such as narrow absorption band, poor Stoke's shift, low quantum efficiency and rapid degradation negatively impact the performance of LSC panels. We mitigate losses from narrow-band absorption and self-absorption due to poor Stoke shift by adopting a face-mounted design for PV cells in the LSC panels. Filtering effects of the dye are reduced by collecting a portion of the incident light through direct illumination on the PV cells[9–11]. Self-absorption increases with photon exposure time to the luminescent material. Flexibility in PV cell placement for face-mounted cells enables faster collection of captured photons. This is further helped by separating the LSC panel into a thin luminescent absorbing layer attached to the back of a thick waveguide, thereby extending the mean-free-path between absorption events. This design comes at the cost of reduced concentration factors and an increase in the amount of PV material used

High and Low Concentrator Systems for Solar Electric Applications VIII, edited by Adam P. Plesniak,
Proc. of SPIE Vol. 8821, 882103 · © 2013 SPIE · CCC code: 0277-786X/13/$18 · doi: 10.1117/12.2024676

when compared with cells mounted on the side, but with rapidly declining PV cell cost, the overall cost per watt power generated is still favorable. Here, we present a study of the LSC panels using Mont-Carlo simulation[12–14] to aid in the design and performance optimization of the panels.

The power gain (γ_{pwr}) as used in this paper is defined as:

$$\gamma_{pwr} = \frac{Power_{panel}}{Power_{ctrl}} = \frac{V_{LSC} \times I_{LSC} + V_{PV} \times I_{PV}}{V_{PV} \times I_{PV}} \quad (1)$$

where V is the open circuit voltage (V_{oc}) and I the short circuit current (I_{sc}). Subscripts panel and ctrl refer to the LSC panel and reference PV cell respectively. This figure measures the change in output power attributed to the addition of a luminescent layer to the panel. The control consists of cells with equivalent PV area attached to clear waveguides in the same configuration as the LSC. Fill factors for all PV cells used are taken to be equal and this was later confirmed by measurement results.

2. MONTE-CARLO RAY TRACING SIMULATION

The simulation model consists of a layered arrangement as shown in Figure 1. An acrylic waveguide makes up the entire top layer of the panel. The second layer is segmented into regions of PV cells interspaced with thin acrylic, infused with LR305 (lumogen red) absorbers. Below each PV cell, a small air gap region is added to compensate for the difference in thickness between the PV cell and absorber layer and to account for circumstances when photons refract out of the absorber layer and travel beneath the PV cell. The number of PV cells, their placement and orientation can all be adjusted to model different panel layouts. Additional layers or dyes can also be added to simulate multi-layer or multi-dye LSC panels.

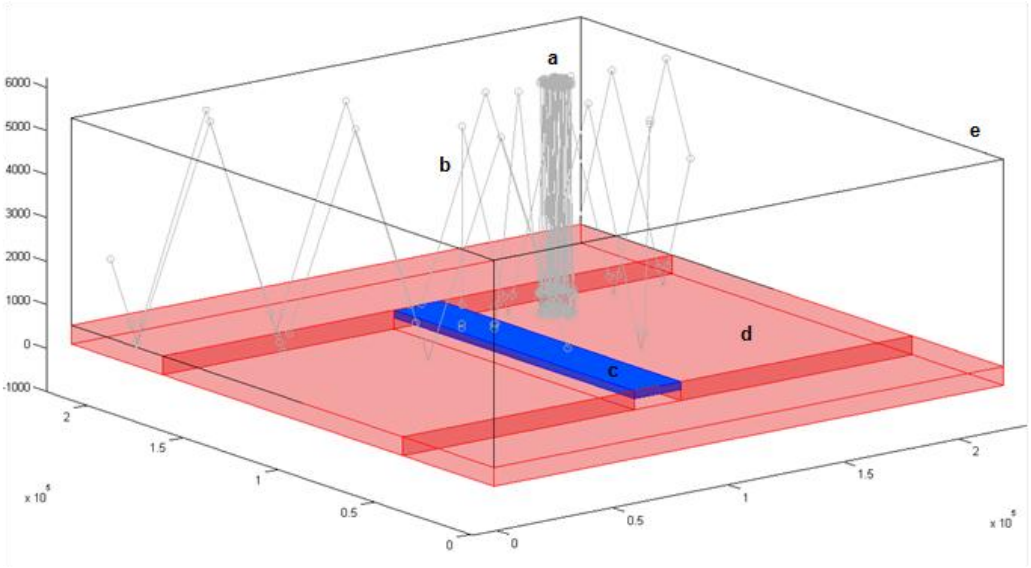

Figure 1. Schematic of the LSC panel with 100 incident photons. a: Incident photon; b: Wave-guided photon; c: PV cell; d: Luminescent layer; e: Waveguide

Photons are launched singly at the LSC panel with the simulation tracking and recording its path and interaction until the photon run is terminated by either escaping the waveguide, lost through non-radiative absorption or when it is collected by a PV cell. Solar radiation contains a highly non-uniform distribution of wavelengths in its spectrum. As photon interactions and free-path length within the LSC panel are dependent on its wavelength, a weighted Monte-Carlo algorithm is applied to reflect this biased probability in the distribution. Each new photon simulation is assigned a direction and random initial starting position. At the start of each movement phase, the photons position within the panel

is first determined. This allows the program to detect if boundary collision or some other interaction has occurred within the panel and apply the appropriate properties and actions unique to each region type as shown in the ray-tracing algorithm (Figure 2). At refractive interfaces, the Fresnel equation is used to calculate a reflection coefficient. In accordance with the Monte-Carlo method, the outcome of each event is decided by comparing calculated probabilities with randomly generated numbers. For photons collected at the PV cell, only photons striking the top of the cell and possessing sufficient energy to generate photon current count towards γ_{pwr} calculations. The mean-free-path of photons within each layer type is calculated using transmission measurements taken and applying the Beer-Lambert law given as:

$$MFP = \left| \frac{t}{\ln[T(\lambda)]} \right| \tag{2}$$

where t = thickness of sample and T(λ)=transmission level measured for each wavelength.

This value is recalculated each time the photon undergoes a wavelength change.

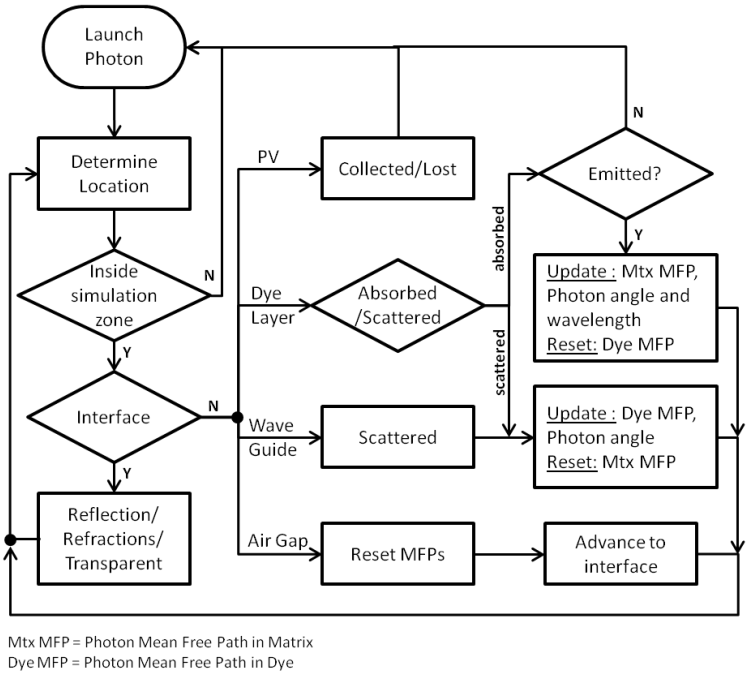

Figure 2. Ray-tracing algorithm flow chart. Photon interactions at interface/boundaries between regions are taken differently from those within the region. Determining the photons' location at the start of the loop allows for the application of the appropriate properties and actions in each layer during each simulation iteration.

3. SIMULATION RESULTS

Because the PV cells are attached front-facing on the LSC panel, there are several structural parameters that can be adjusted to improve γ_{pwr} which are absent in a panel with side-mounted PV cells.

3.1 Waveguide thickness dependence

As illustrated in Figure 3, waveguide thickness directly impacts the distance photons travel free of interaction with the absorbing layer. The objective here is to minimize reabsorption probability by transporting photons trapped in the waveguide efficiently to the PV cells for collection with the minimum number of passes through the absorbing layer. For each dye absorption event, there is a chance that no re-emission will take place. On top of that, emission is isotropic and there is a chance that the photon will be emitted within the escape cone by which it will not undergo total internal

reflection and exit the waveguide. In front-facing LSC designs, there exists for each PV cell size, a range of matched waveguide thickness that produces the fewest reabsorption events and their associated losses.

Simulation results (Figure 3) for a single 1x12.5 cm or 2x12.5 cm PV cell demonstrates the above idea showing a distinct range of waveguide thickness that result in the largest percentage of trapped photons collected by the PV cell.

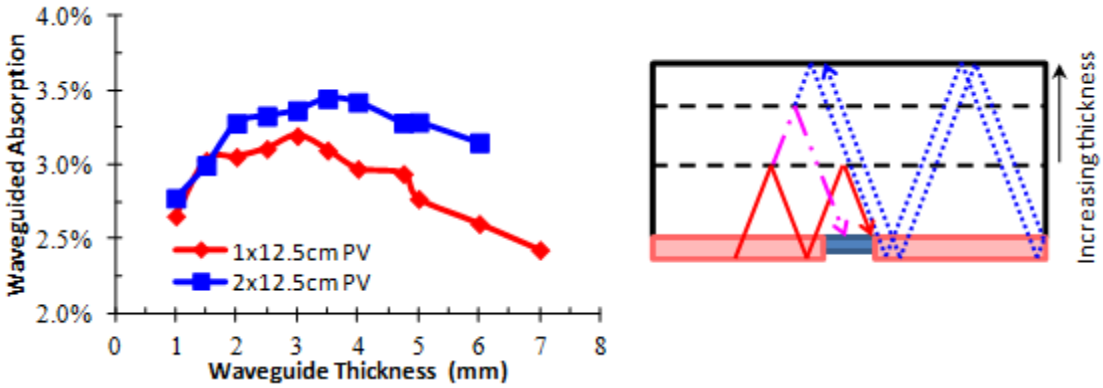

Figure 3. Percentage of photons collected by PV cell through waveguiding action versus the waveguide (acrylic) thickness for a single 1x12.5cm or 2x12.5 cm wide cell

3.2 Separation between PV cells

The ratio of luminescent absorber area to PV area for a fixed panel size is variable depending on the cost, power outputs and concentration factors desired. But while high absorber to PV ratios raise the concentration factor and hence γ_{pwr}, we also aggravate reabsorption and scattering losses as photons collected further out travel a long path to reach the PV cell. The question then is, if and when this gain in γ_{pwr} is offset by increasing losses. This design parameter is highly dependent on the concentration of luminescent dye used, its quantum efficiency and stoke shift of the dye. The result is also affected to a degree by the waveguide thickness as discussed in the previous sub-section.

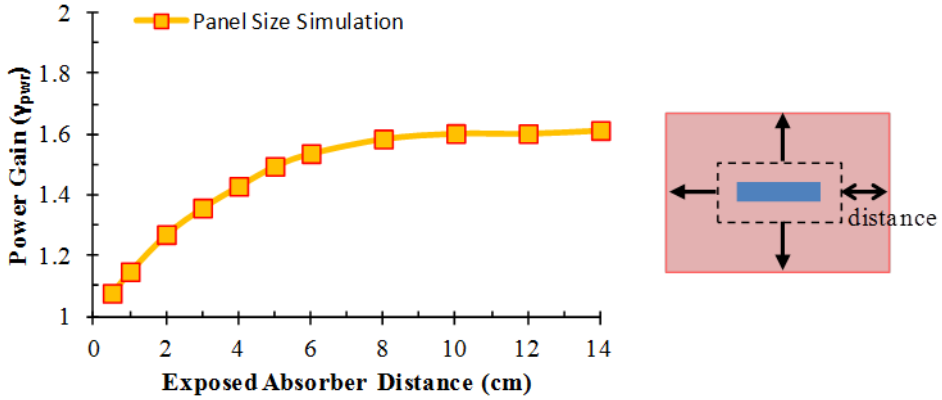

Figure 4. Power gain versus the size of LSC panel. Illumination angle is 0 degrees from the plane normal.

From the graph shown in Figure 4, we see a liner initial increase in γ_{pwr} with absorber area which begins to taper off when the absorber material extends out approximately 6cm from the PV cell edge. This corresponds to the average distance emitted photons are able to travel freely in the LSC panel without experiencing any matrix scattering or reabsorption. Larger panels see their γ_{pwr} improvements decline sharply and with this, we can see that any additional area added is a waste of the space and material expended. This data translates to what the optimal spacing between adjacent

cells should be on the LSC panel. To verify that simulation results are good representations of actual LSC panel performances, a masking experiment was carried out using a large panel with unwanted areas masked by off by opaque boards and masking tape. Measurements were taken in the month of September at approximately 2-3pm giving an incidence angle of approximately 42°. Simulations of the panel match the experimental results well with an offset of approximately 0.18 as shown in Figure 5.

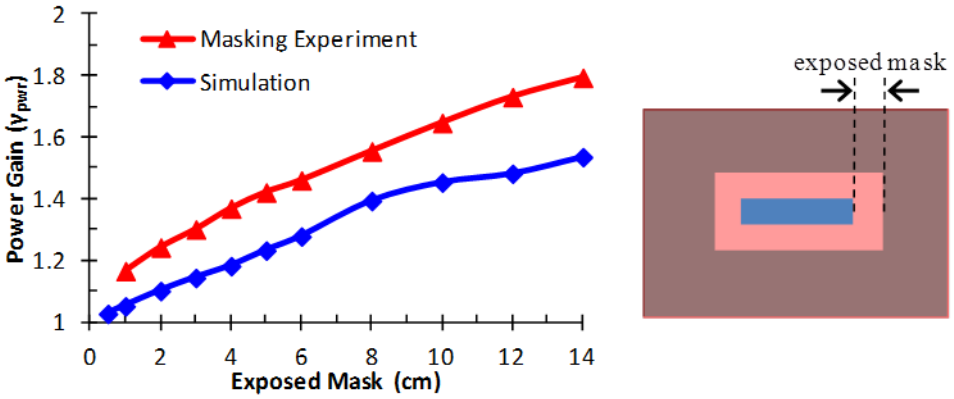

Figure 5. Power gain versus the amount of exposed LSC, comparing experimental (triangle) and simulation (diamond) results. Illumination angle is 42 degrees from the plane normal.

3.3 Panel layout

We next turn to cell placement as an optimizing parameter. As with the previous subsections, addressing reabsoption, scattering and efficient transport of trapped photons to collection centers are the primary target of this study. The isotropic emission from the dyes can end up with photons emitted in certain angles experiencing greatly increased travel time and distance in the LSC panel even with the cell to cell spacing derived in section 3.2. In Figure 6b, we have the top view of two identical LSC panels differing only in the arrangement of PV cells. It was proposed that for the 'Inline' arrangement in Figure 6bii, photons emitted in horizontal directions approximately parallel to the string of PV cells might end up travelling multiple times across the LSC panel before finally arriving at a PV cell. The 'ZigZag' pattern in Figure 6bi attempts to nullify this by breaking up the PV cell string in order to minimize this travel distance regardless of the horizontal emission angle.

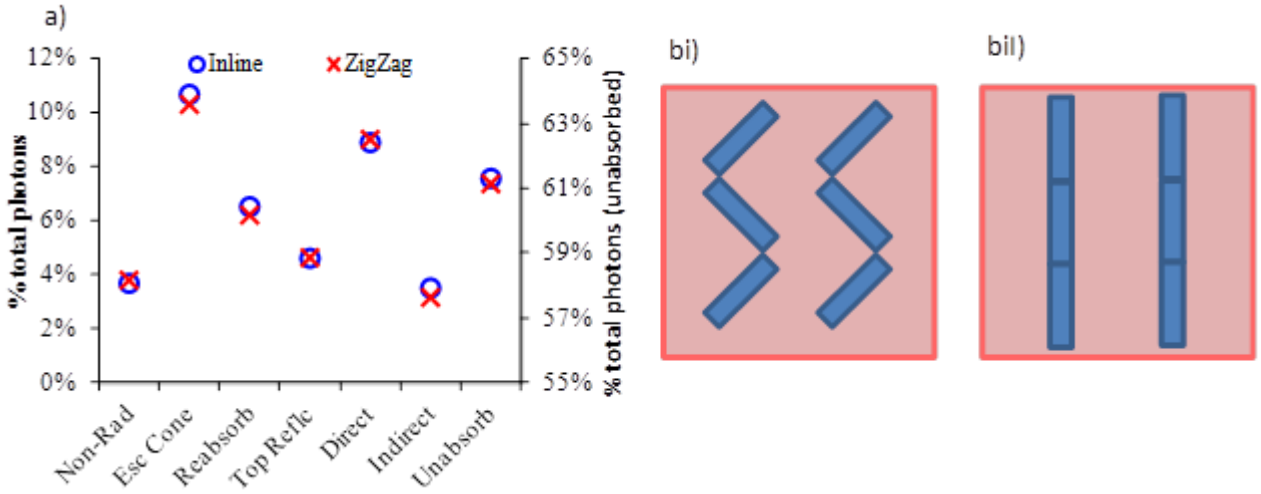

Figure 6. a) Comparing photon distribution in zigzag and inline arrange cells b) ZigZag (i) and Inline(ii) ell arrangements with the same exact panel area and PV cell coverage.

Comparing the photon distribution in both panels (Figure 6a), a decrease in escape cone and reabsorption losses when switching to the 'ZigZag' pattern is seen but the differences are so slight that they are effectively negligible. This result is contrary to what was expected. Spacing between columns could be a factor affecting the result and more PV cell arrangements can be explored to further reduce the losses incurred.

3.4 Loss mechanisms

In analyzing the distribution of photon losses incurred in the LSC panel (Figure 7), approximately 65% of photons incident pass through unabsorbed, a result of the single dye system that was used and the narrow absorption range of the dye. Depending on the application, this outcome could be desired for instance in green house applications where we would only want to extract the wavelengths unused by plants for photosynthesis and growth. Other significant losses come from the luminescent dye emitting light into the escape cone and increased reabsorption that comes with larger panel sizes. While escape cone losses might lessen with higher refractive index waveguides used, this is also accompanied by increase Fresnel reflection off the top of the waveguide reducing the amount of both direct and specular light collected at the PV cell. Top reflection and non-radiative absorption account for losses of 4% each. Top reflection could be addressed via applying a broad band anti-reflection coating to the top surface. Modifying the top surface by adding a lens or scattering layer could induce more light to enter the panel provided it does not disrupt the waveguide properties and cause more light to escape from within.

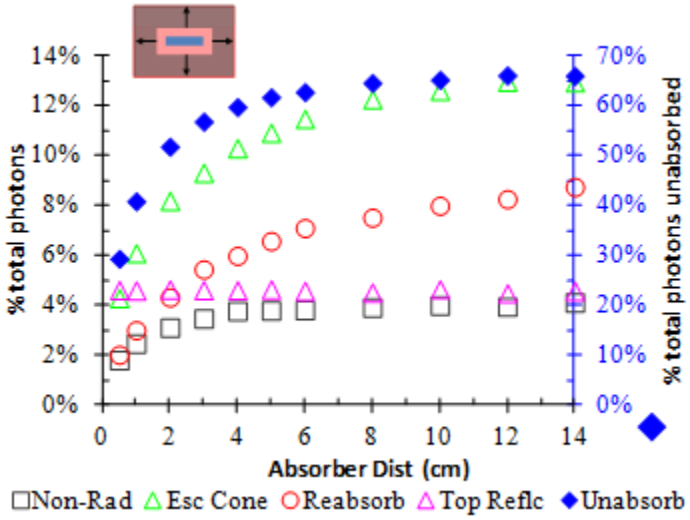

Figure 7. Distribution of photon losses versus panel size. Any loss resulting from multiple absortion events are grouped into the Reabsorb category.

4. CONCLUSION

In summary, a three dimensional Monte-Carlo ray-tracing model was developed to facilitate the study of LSC panels with front-facing PV cells and speed up the design optimization process. Panel dimensions and PV cell placement and area coverage can be predicted for optimal panel performance. Thus far we have considered only the effects of these variables on the power gain (γ_{pwr}) of the panel. Other factors such as the cost per watt generated or total power output may skew the results presented in preceding sections to achieve their goal. Scrutinizing the photon loss distribution in the panel highlight areas to be addressed in future design.

REFERENCES

[1] Norton, B., Eames, P.C., Mallick, T.K., Huang, M.J., McCormack, S.J., Mondol, J.D., and Yohanis, Y.G., "Enhancing the performance of building integrated photovoltaics," Solar Energy 85(8), 1629–1664 (2011).

[2] Chemisana, D., "Building Integrated Concentrating Photovoltaics: A review," Renewable and Sustainable Energy Reviews 15(1), 603–611 (2011).

[3] Wiegman, J.W.E., and van der Kolk, E., "Building integrated thin film luminescent solar concentrators: Detailed efficiency characterization and light transport modelling," Solar Energy Materials and Solar Cells 103(0), 41–47 (2012).

[4] Richards, B.S., "Enhancing the performance of silicon solar cells via the application of passive luminescence conversion layers," Solar Energy Materials and Solar Cells 90(15), 2329–2337 (2006).

[5] Slooff, L.H., Bende, E.E., Burgers, A.R., Budel, T., Pravettoni, M., Kenny, R.P., Dunlop, E.D., and Büchtemann, A., "A luminescent solar concentrator with 7.1% power conversion efficiency," physica status solidi (RRL) - Rapid Research Letters 2(6), 257–259 (2008).

[6] Sark, W.G.J.H.M. van, Barnham, K.W.J., Slooff, L.H., Chatten, A.J., Büchtemann, A., Meyer, A., McCormack, S.J., Koole, R., Farrell, D.J., et al., "Luminescent Solar Concentrators - A review of recent results," Optics Express 16(26), 21773–21792 (2008).

[7] Klampaftis, E., Ross, D., McIntosh, K.R., and Richards, B.S., "Enhancing the performance of solar cells via luminescent down-shifting of the incident spectrum: A review," Solar Energy Materials and Solar Cells 93(8), 1182–1194 (2009).

[8] Strümpel, C., McCann, M., Beaucarne, G., Arkhipov, V., Slaoui, A., Švrček, V., del Cañizo, C., and Tobias, I., "Modifying the solar spectrum to enhance silicon solar cell efficiency—An overview of available materials," Solar Energy Materials and Solar Cells 91(4), 238–249 (2007).

[9] Corrado, C., Leow, S.W., Osborn, M., Chan, E., Balaban, B., and Carter, S.A., "Optimization of gain and energy conversion efficiency using front-facing photovoltaic cell luminescent solar concentratordesign," Solar Energy Materials and Solar Cells 111, 74–81 (2013).

[10] Reisfeld, R., Eyal, M., Chernyak, V., and Zusman, R., "Luminescent solar concentrators based on thin films of polymethylmethacrylate on a polymethylmethacrylate support," Solar Energy Materials 17(6), 439–455 (1988).

[11] Mansour, A.., "On enhancing the efficiency of solar cells and extending their performance life," Polymer Testing 22(5), 491–495 (2003).

[12] Carrascosa, M., Unamuno, S., and Agullo-Lopez, F., "Monte Carlo simulation of the performance of PMMA luminescent solar collectors," Applied Optics 22(20), 3236–3241 (1983).

[13] Burgers, A., Slooff, L., Kinderman, R., and Van Roosmalen, J., "Modelling of luminescent concentrators by ray-tracing," in Presented at the 20th European Photovoltaic Solar Energy Conference and Exhibition 6, 10 (2005).

[14] Schüler, A., Kostro, A., Galande, C., Valle del Olmo, M., Chambrier, E., and Huriet, B., [Principles of Monte-Carlo Ray-Tracing Simulations of Quantum Dot Solar Concentrators] , in Proceedings of ISES World Congress 2007 (Vol. I – Vol. V), D. Y. Goswami and Y. Zhao, Eds., Springer Berlin Heidelberg, 1033–1037 (2009).